

# Embrittlement of a Duplex Stainless Steel in Acidic Environment Under Applied Cathodic Potentials

S. Roychowdhury and Vivekanand Kain

(Submitted February 22, 2007; in revised form September 18, 2007)

**Hydrogen-induced degradation of mechanical properties of a duplex stainless steel in 0.1N H<sub>2</sub>SO<sub>4</sub> solution has been studied under in situ cathodic charging conditions. Significant reductions in percentage of elongation, toughness, and time to failure were noticed due to the ingress of hydrogen into the material at various applied cathodic potentials in the range of –200 to –800 mV (SCE). Cleavage fractures were identified mainly in the ferritic phases. Crack growth was observed to be inhibited by the austenite phase. However, depending on the severity of the environment, both the ferrite and austenite phases could be embrittled. At less negative potentials, presence of surface film and low hydrogen fugacity seemed to control hydrogen ingress in the metal. Addition of thiosulfate to the acidic solution further degraded the mechanical properties of the steel at the applied cathodic potential.**

**Keywords** ductility, duplex stainless steel, fracture, hydrogen embrittlement, toughness

## 1. Introduction

Duplex stainless steels (DSSs) containing both austenite and ferrite are being increasingly used in many industries such as oil, gas, and petrochemical industries. At present, a variety of duplex stainless steels are available which are far better than many single-phase austenitic or ferritic stainless steels in terms of resistance to localized corrosion as well as stress corrosion cracking (SCC). *Strength of these steels is higher than the single-phase austenitic stainless steels.* However, in many applications, duplex stainless steels are expected to face harsh environments which may contain Cl<sup>-</sup>, H<sub>2</sub>S, and CO<sub>2</sub> and the operating temperature also may be as high as 200 °C.

Various electrochemical reactions may take place on the duplex stainless steel surfaces in the above environments, particularly the cathodic reactions when in contact with carbon steels which are being protected cathodically by applying potentials in the range of –700 to –800 mV<sub>SCE</sub>. Thus there exists the possibility that the cathodic reactions which produce hydrogen may result in early failure/cracking of these steels by way of hydrogen embrittlement (HE).

Valdez-Vallejo et al. (Ref 1) reported that duplex stainless steels having an appropriate austenite/ferrite-phase ratio would not be susceptible to HE in seawater even under conditions of cathodic overprotection. They stated that this was because, firstly, the stress level would not approach the tensile strength and, secondly, even if some microscopic cracks were initiated at lower stress levels, they would be prevented from cracking

by the austenite phases. However, several other researchers (Ref 2–4) have observed HE in DSS by carrying out different tests including slow strain rate tests and reported the dependency of this embrittlement on strain rate, electrode potential, hydrogen partial pressure, etc. Marrow et al. (Ref 5, 6) and Krishnan (Ref 7) reported hydrogen-assisted fatigue failure of DSSs in both hydrogen gas and 3.5% NaCl solution.

Like other stainless steels, duplex stainless steels are also protected from corrosion in many environments by a passivating film present on the surface. This passivating film may influence not only the corrosion behavior, but also the hydrogen ingress into the metal in different environments. The objective of this investigation was to evaluate the effects of applied cathodic potentials on the mechanical properties of a DSS under slow strain rate test (SSRT) condition in one acidic environment/solution and to characterize the fracture surfaces in the austenite and ferrite grains in terms of the ductile and brittle failures.

Thiosulfate depolarizes the hydrogen evolution reaction and increases the hydrogen permeation rate in metals. Thus, the effect of thiosulfate in the above experiments was also looked into.

## 2. Experimental

The composition of the DSS used in this study was C-0.023, Cr-22.17, Ni-4.73, Mo-2.73, Mn-1.19, Si-0.77, P-0.027, S-0.002, N-0.12, Fe-bal (wt.%).

The initial material was in the form of a 12-mm thick plate from which round tensile specimens having 25-mm gauge length and 4-mm diameter were machined. The specimens were then annealed at 1100 °C for 15 minutes and water quenched. Before each test, the specimens were ground with 600-grade emery paper in the longitudinal direction and then cleaned with acetone. During the tests, the specimens were pulled at a slow strain rate of 10<sup>-6</sup> s<sup>-1</sup> while being cathodically charged in situ at various potentials in 0.1N H<sub>2</sub>SO<sub>4</sub> solution of pH 1.4. To find

S. Roychowdhury and Vivekanand Kain, Materials Science Division, Bhabha Atomic Research Centre, Trombay, Mumbai 400085, India. Contact e-mail: supratik@barc.gov.in.

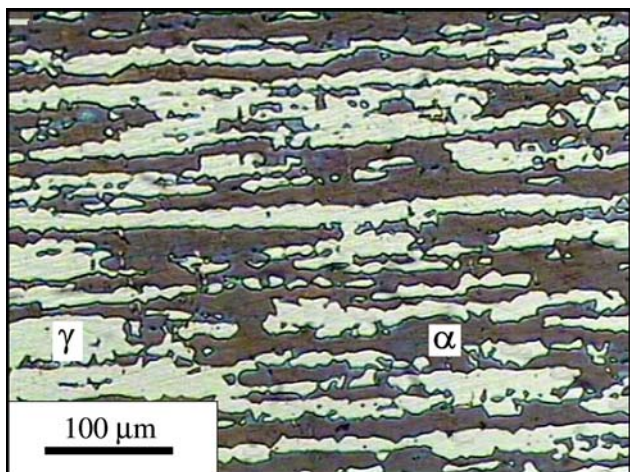


Fig. 1 Microstructure of annealed DSS

the effect of thiosulfate, 10-20 mM sodium thiosulfate was added to the  $H_2SO_4$  (0.1N) solution and the slow strain rate tests (SSRT) were conducted applying the same strain rate as above. All the experiments were carried out at room temperature and the solution was exposed to the atmosphere during the experiment.

The specimen potentials were measured with respect to a saturated calomel electrode (SCE) and the specimens were charged cathodically up to a potential of  $-800$  mV. The fracture surfaces of the failed samples were examined under SEM to investigate the mode of fracture.

### 3. Results

#### 3.1 Microstructure

The microstructure of the annealed material showed the presence of elongated bands of austenite and ferrite as shown in Fig. 1. Through image analysis, the amounts of austenite and ferrite in the material were found to be 53 and 47%, respectively.

#### 3.2 SSRT Under Applied Potentials

Figure 2 shows the changes observed in the stress-strain curves due to the application of cathodic potentials. There has been gradual decrease in the elongation values with cathodic potentials from  $-200$  to  $-800$  mV. This has been clearly depicted in Fig. 3(a-e), which presents the effects of various applied cathodic potentials on several mechanical properties of the steel under study.

The percentage elongation in air was 36%, whereas at  $-800$  mV, the elongation was reduced to 10%, Fig. 3(a). The proof stress, Fig. 3(b), was reduced from 511 MPa in air to 490 MPa at  $-200$  mV applied potential and thereafter not much reduction could be noticed on further charging at more negative potentials. A similar trend was noticed for the UTS values, Fig. 3(c).

A significant decrease in the percentage reduction in area (%RA) due to the application of cathodic potentials was recorded. In air, the reduction in area for the annealed material was about 54.5%; charging at potentials in the range of  $-200$  to

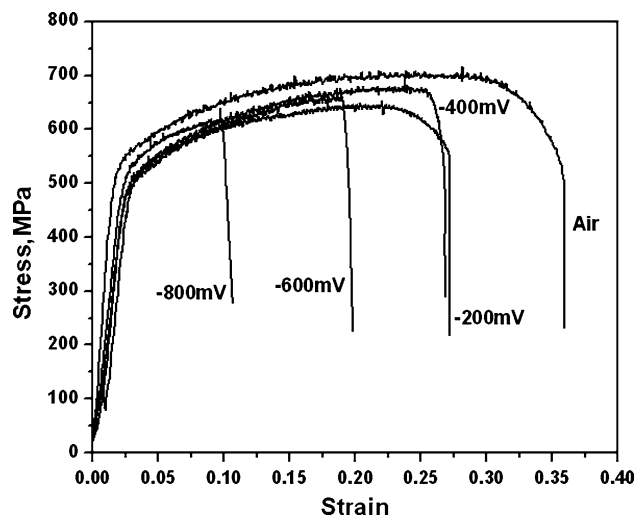


Fig. 2 Stress-strain behavior under different applied cathodic potentials

$-600$  mV reduced it to around 23%. However, when charged at  $-800$  mV, a drastic reduction in %RA took place, which was found to be 13.5%, Fig. 3(d). The area under the stress strain curve is a good measure of toughness of any material. Figure 3(e) shows the toughness values, thus measured, at different applied potentials. Significant reduction in toughness was noticed with the application of negative potentials.

The time taken by specimens to fail (TTF) at negative potentials has been presented in Fig. 4. At  $-200$  mV, the TTF was 85 h, whereas at  $-800$  mV, specimens failed within 32 h.

#### 3.3 Effects of Thiosulfate Addition

As shown in Fig. 3(a-e), it may be noted that addition of 10 and 20 mM  $Na_2S_2O_3$  to 0.1N  $H_2SO_4$  solution further degraded the mechanical properties of the DSS and also correspondingly reduced the time to failure of specimens, Fig. 4. At  $-800$  mV, specimens failed within 32 h in the absence of thiosulfate. However, presence of thiosulfate reduced the time to failure to around 25 h at the same applied potential of  $-800$  mV.

#### 3.4 Fractography

Specimens tested in air showed ductile fracture. Consequently ductile dimples were noticed on the fracture surface, as shown in Fig. 5.

Cracks, formed on the surface of the specimens which were charged cathodically, were examined under optical microscope. It was observed that cracks mostly originated at the ferrite grains, Fig. 6.

However crack growth was inhibited as and when the cracks encountered an austenite grain as depicted in Fig. 7. It may be noted here that it is one of the mechanisms which make duplex stainless steels more resistant to crack growth than the single-phase stainless steels in less severe environments, and when a crack meets the softer-phase austenite, it stops further growing.

Under the SEM, transgranular cleavage in the ferrite phase was observed to be the predominant mode of fracture of this steel during cathodic charging, whereas plastic deformation was involved with the austenite phase as shown in Fig. 8 which shows the presence of austenite ligaments along with cleavage facets in ferrite. Ductile tearing of the austenite phase could

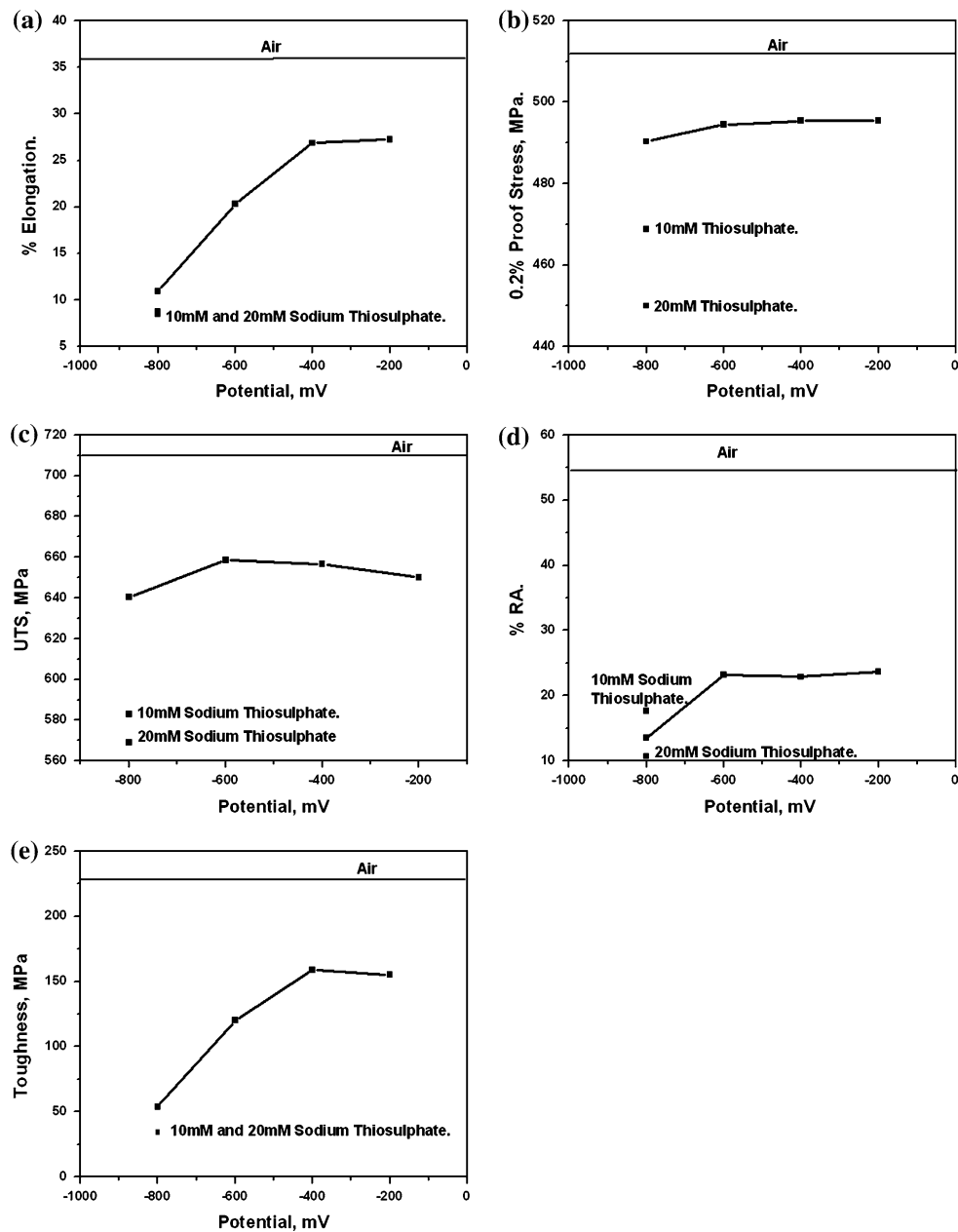


**Fig. 3** Variations in (a) %elongation, (b) 0.2% Proof stress, (c) UTS, (d) %Reduction in area and (e) Toughness, with different applied cathodic potentials

further be noticed in between the ferrite cleavage facets in Fig. 9. Presence of cleavage facets in both the austenite and ferrite phases was also noticed at places on the fracture surface as a result of hydrogen charging, as shown in Fig. 10.

#### 4. Discussion

Surface films present or produced on stainless steels in any environment play a dominant role in controlling not only the general corrosion behavior but also localized corrosion, such as pitting, SCC, and HE as well. In low pH acidic solutions, such surface films are expected to be less protective. El-Yazgi and Hardie (Ref 8) reported *high* ductility of a DSS in both NACE

standard solution as well as in 3.5% NaCl solution (pH 3.2) at low temperatures (<30 °C) as compared to that at higher temperatures (~30 to 50 °C). They concluded that the *reduced* embrittlement at the lower temperatures could be attributed to *the prevention of hydrogen entry by the formation of some form of a protective film*. Banerjee and Chatterjee (Ref 9), who measured the hydrogen concentrations in HSLA-80 steel after charging in synthetic seawater at different cathodic potentials, reported that the decrease in hydrogen concentration beyond -1000 mV was due to the formation of a surface film. Thus, it is expected that HE of DSSs will also depend on the presence or absence as well as the type of surface/passive film which may form due to their exposure to various environments, acidic or alkaline and also containing chlorides, sulfides, etc. In fact, as shown by the polarization diagram in Fig. 11, a surface film

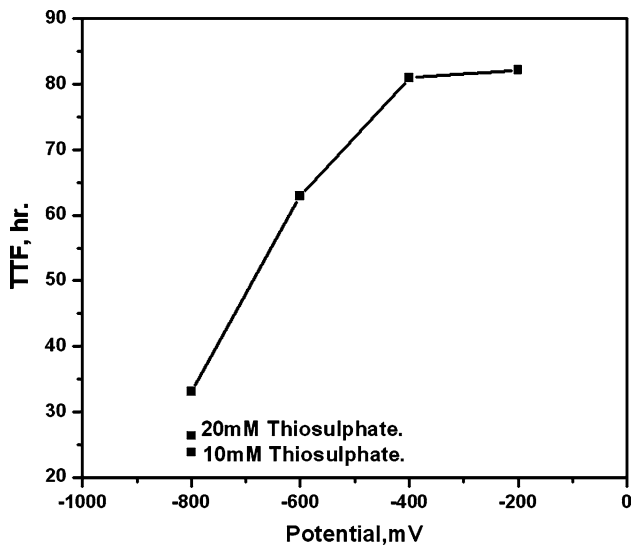


Fig. 4 Variation in TTF with applied potential

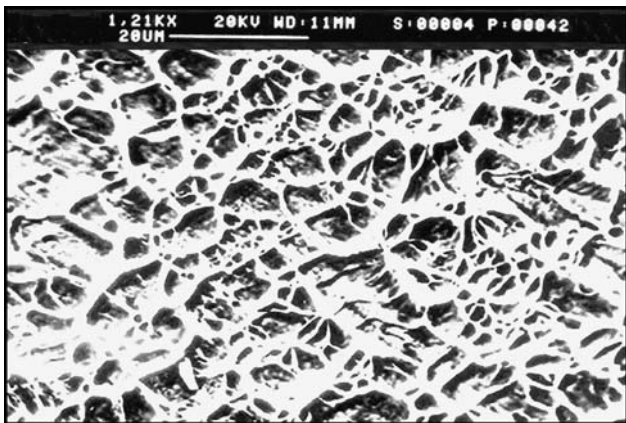


Fig. 5 Ductile failure in air

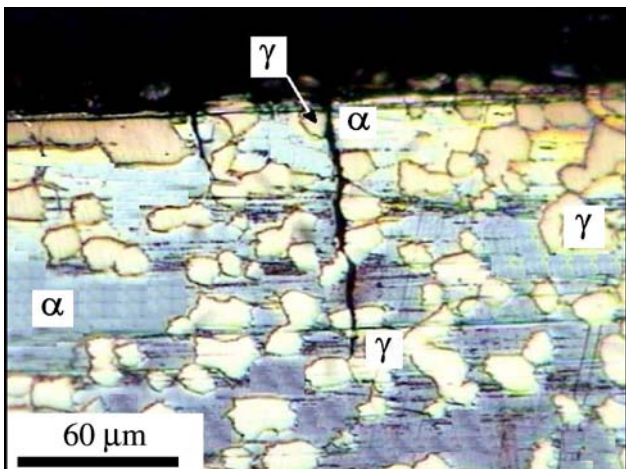


Fig. 6 Initiation of cracks at the ferrite phase

does form and exists on the DSS in 0.1N H<sub>2</sub>SO<sub>4</sub> solution. *There is no active/passive transition and the passive film formation starts at potentials anodic to the open circuit potential.*

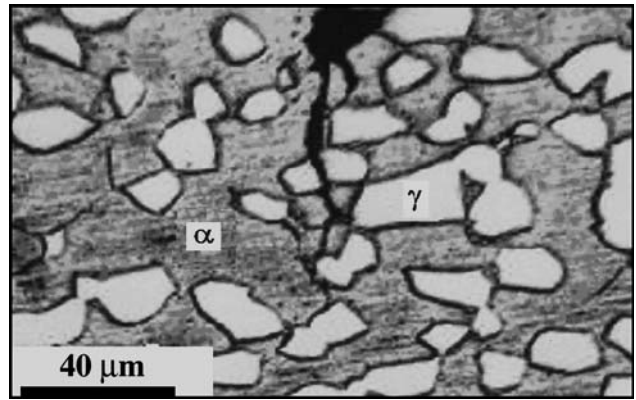


Fig. 7 Picture showing growth of a crack through austenite and ferrite phases and crack arrest at austenite phase

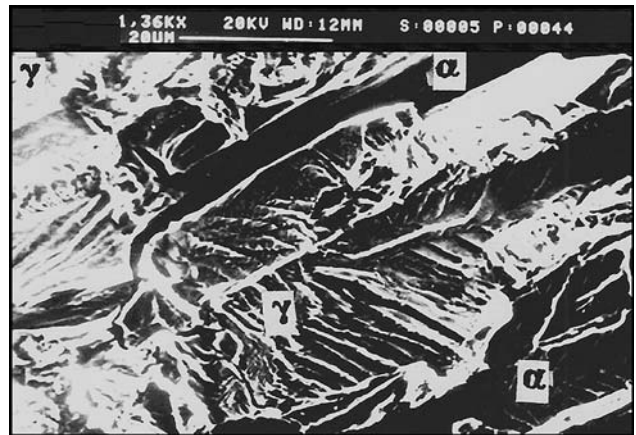


Fig. 8 SEM fractograph showing cleavage fracture in ferrite phases and ductile tearing of austenite phases



Fig. 9 Ductile tearing of austenite phase present in between ferrite cleavage facets

In the present investigation, it was clearly observed that in low pH acidic solution, 0.1N H<sub>2</sub>SO<sub>4</sub>, the DSS, under study, suffered a significant loss in ductility and toughness due to hydrogen ingress when cathodically polarized at negative potentials. The percentage of elongation was reduced from

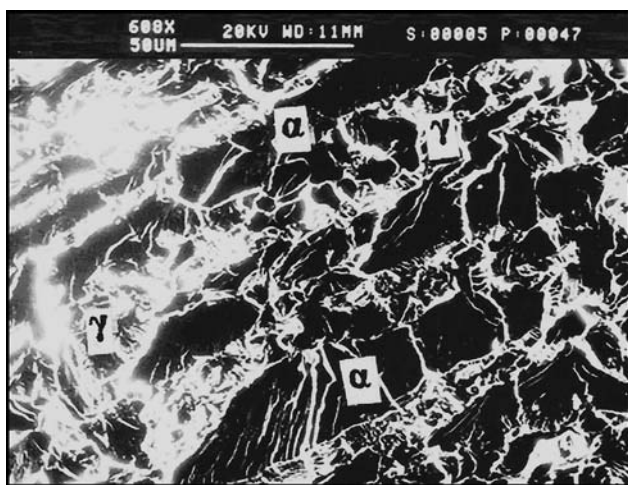


Fig. 10 Cleavage facets in both austenite and ferrite phases

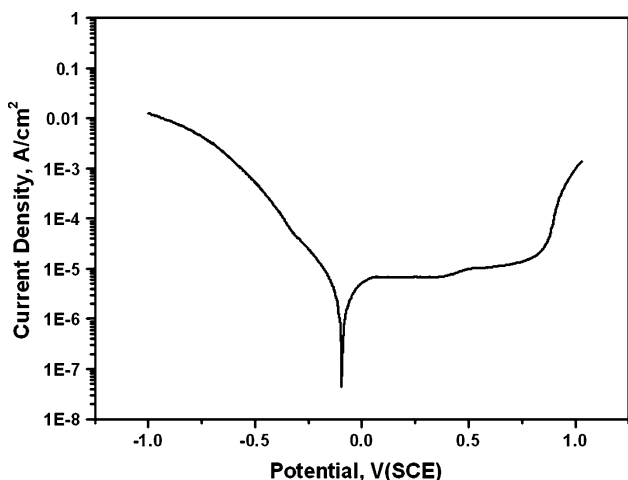


Fig. 11 Electrochemical polarization diagram of DSS in 0.1N  $H_2SO_4$  solution

36% in air to 10% in the solution at  $-800$  mV. Hydrogen produced at different applied negative potentials could diffuse inside the material and result in embrittlement of the steel. However, the availability of hydrogen or the hydrogen fugacity and also the actual surface conditions, as discussed above may control the degree of embrittlement. In such acidic solutions, hydrogen activity will be more as compared to other non-acidic solutions and also hydrogen fugacity will be appreciable at negative potentials. Because of these reasons, the degree of embrittlement gradually increased with the increase in potentials in the negative direction, from  $-200$  to  $-800$  mV. Presence of surface film and low hydrogen fugacity at  $-200$  mV might have resulted in the reduced embrittling effect as compared to the effects seen at more negative potentials.

Though there was almost continuous decrease in elongation and toughness from  $-200$  mV to  $-800$  mV, the proof stress and UTS values were reduced to lower values at  $-200$  mV itself and thereafter not many changes in these values were recorded. It is expected that the concentration of hydrogen in

the metal will increase with the application of more negative potentials (Ref 10, 11); however, it has been shown by some workers (Ref 12, 13) that a critical hydrogen concentration is required to initiate damage/cracking in the metal. Such a critical hydrogen concentration seemed to have been achieved at  $-200$  mV at which potential the present steel has shown a drastic reduction in all the mechanical parameters. The constancy in the stress values beyond  $-200$  mV may be explained by the pinning of edge dislocations by hydrogen atoms, thus not allowing the proof stress to decrease further. A similar effect may at times increase the yield strength/proof stress in case of other metals as has been observed by some workers (Ref 14, 15). The constancy in the UTS values could also be explained by the hydrogen-dislocation interaction which may result in decreased movement of screw dislocations, thus restricting cross slip, as reported by Oriani and Josphie (Ref 14).

The fractographic observations were found to commensurate with the results of cathodic charging. Crack initiation was through ferrite phase and also extensive cleavage fracture was noticed in the same phase with ductile tearing of the austenite. Though austenite has higher solubility for hydrogen than that in the ferrite phase, hydrogen diffusivity is higher in the ferrite phase. Owczarek and Zakroczymski (Ref 16) reported hydrogen diffusivity for the ferrite and austenite phases in a DSS containing 40% austenite as around  $1.5 \times 10^{-11}$  and  $1.4 \times 10^{-16}$   $m^2/s$ , respectively. In fact hydrogen transport in duplex steels is a very complicated process because of this extremely different mobility of hydrogen in the two phases as well as trapping of hydrogen atoms at the ferrite-austenite interface. Experimental analyses (Ref 17, 18) of permeation transients have shown that the effective diffusivity of hydrogen in a DSS containing 44% austenite was reduced by 400 times as compared to that in one fully ferritic steel and also that trapping of hydrogen atoms at the ferrite-austenite interface was a significant factor in reducing the diffusivity. However, hydrogen could diffuse quickly in the ferrite phase, resulting in its embrittlement. As shown in Fig. 11, cleavage facets in the austenite grains were also detected. Thus, depending on the severity of the environment, both the phases could be embrittled by hydrogen.

Some of the cracks in the specimen were followed up to the place where they had stopped growing. Most of these cracks, shown in Fig. 7, were found to have stopped growing as and when they met an austenite grain. This is called the keying effect when a crack in DSSs stops further growing as it meets the softer phase austenite.

Thiosulfate is known to promote hydrogen ingress in metals and is commonly encountered in the pulp, paper, oil and gas industries. It may also be produced by sulfate reducing bacteria. Thus, it becomes important to find the effect of thiosulfate on the hydrogen embrittlement characteristics of DSSs. In the present investigation, presence of thiosulfate in the 0.1N  $H_2SO_4$  solution has been observed to be very detrimental as it further accelerated the embrittling effect of hydrogen at  $-800$  mV. Abd Elhamid et al. (Ref 19) reported that thiosulfate promoted hydrogen evolution and permeation in iron in both acidic and neutral solutions and they attributed its effect mainly to its decomposition products like  $H_2SO_3$ ,  $HSO_3^-$ ,  $SO_3^-$ , and colloidal sulfur, since thiosulfate is readily decomposed in acidic media to give the above products. Thus, the presence of thiosulfate in acidic or neutral solutions is expected to further degrade the mechanical properties of DSSs as far as HE is concerned.

## 5. Conclusions

- (1) Depending on the magnitude of applied cathodic potentials, duplex stainless steels may be severely embrittled due to the ingress of hydrogen into the steel in the acidic solutions. Considerable reduction in mechanical properties of a duplex stainless steel has been observed in this investigation as a result of HE consequential to cathodic hydrogen charging.
- (2) Initiation of cracks was mostly associated with ferrite phases. Cracks were identified to have stopped growing once they encountered austenite grains.
- (3) Transgranular cleavage in the ferrite phase was the primary mode of fracture. The presence of austenite ligaments on the fracture surface indicated ductile mode of failure of this phase, though small cleavage facets were present at places in the austenite phase.
- (4) Proper care must be taken while cathodically protecting carbon steels which are in contact with duplex stainless steels. Application of cathodic potentials may render DSSs prone to HE.
- (5) Presence of thiosulfate further degraded the mechanical properties of the DSS at the applied cathodic potential.

## Acknowledgment

The authors express their gratitude to Dr. G.K. Dey, Head, Materials Science Division and Dr. S. Banerjee, Director, Bhabha Atomic Research Centre, for their encouragement and useful suggestions during the course of this investigation.

## References

1. J.R. Valdez-Vallejo, R.C. Newman, and R.P.M. Procter, Proc. 4th Intl. Conf. on "Effect of Hydrogen on the Behavior of Materials", Moran, WY, 1989, p 1003
2. T.P. Perng and C.J. Altstetter, Cracking Kinetics of Two-phase Stainless Steel Alloys in Hydrogen Gas, *Metall. Trans.*, 1988, **19A**, p 145–152
3. W. Zheng and D. Hardie, The Effect of Hydrogen on the Fracture of a Commercial Duplex Stainless Steel, *Corros. Sci.*, 1991, **32**, p 23–36
4. F. Elsawesh and J.C. Scully, Hydrogen Embrittlement of 22-5 Duplex Stainless Steel, *Br. Corros. J.*, 1998, **33**, p 49–52
5. T.J. Marrow, C.A. Hipsley, and J.E. King, Effect of Mean Stress on Hydrogen Assisted Fatigue Crack Propagation in Duplex Stainless Steel, *Acta Metall. Mater.*, 1991, **36**, p 1367–1376
6. T.J. Marrow and J.E. King, Microstructural and Environmental Effects on Fatigue Crack Propagation in Duplex Stainless Steels, *Fatigue Fract. Eng. Mater.*, 1994, **17**, p 761–771
7. K.N. Krishnan, Mechanism of Corrosion Fatigue in Super Duplex Stainless Steel in 3.5 percent NaCl Solution, *Int. J. Fract.*, 1997, **88**, p 205–213
8. A.A. El-Yazgi and D. Hardie, Stress Corrosion Cracking of Duplex and Super Duplex Stainless Steels in Sour Environments, *Corros. Sci.*, 1998, **40**, p 909–930
9. K. Banerjee and U.K. Chatterjee, Hydrogen Embrittlement of an HSLA 80 Steel in Sea Water Under Cathodic Charging Conditions, *Mater. Sci. Technol.*, 2000, **10**, p 517–523
10. M.J. Robinson and P.J. Kilgallon, Hydrogen Embrittlement of Cathodically Protected HSLA Steels in the Presence of Sulphate Reducing Bacteria, *Corrosion*, 1994, **50**, p 626–635
11. Y. Yamaguchi, H. Nonka, and K. Yamakawa, Effect of Hydrogen Content on Threshold Stress Intensity Factor in Carbon Steel in Hydrogen-Assisted Cracking Environments, *Corrosion*, 1997, **53**, p 147–155
12. H.J. Maier, W. Popp, and H. Kaesche, A Method to Evaluate the Critical Hydrogen Concentration for Hydrogen-induced Crack Propagation, *Acta Metall.*, 1987, **35**, p 875–880
13. L. Coedreuse and J. Charles, The Use of a Permeation Technique to Predict Critical Concentration of H<sub>2</sub> for Cracking, *Corros. Sci.*, 1987, **27**, p 1169–1181
14. R.A. Oriani and P.H. Josphic, Effects of Hydrogen on the Plastic Properties of Medium-Carbon Steels, *Metall. Trans.*, 1980, **11A**, p 1809–1819
15. S. Asano and R. Otsuka, The Lattice Hardening due to Dissolved Hydrogen in Iron and Steel, *Scripta Metall.*, 1976, **10**, p 1015–1020
16. E. Owczarek and T. Zakroczymski, Hydrogen Transport in a Duplex Stainless Steel, *Acta Mater.*, 2000, **48**, p 3059–3070
17. A. Turnbull and R.B. Hutchings, Analysis of Hydrogen Atom Transport in a Two-phase Alloy, *Mater. Sci. Eng.*, 1994, **A177**, p 161–171
18. R.B. Hutchings, A. Turnbull, and A.T. May, Measurement of Hydrogen Transport in a Duplex Stainless Steel, *Scripta Metall. Mater.*, 1991, **25**, p 2657–2662
19. M.H. Abd Elhamid, B.G. Ateya, K.G. Weil, and H.W. Pickering, Effect of Thiosulfate and Sulfite on the Permeation Rate of Hydrogen Through Iron, *Corrosion*, 2001, **57**, p 428–432